ISSN 2413-5577, Ecological Safety of Coastal and Shelf Zones of Sea, 2025, No. 4, pp. 76–96.

Original paper

Climatic Variability of the Water Thermohaline Structure in the Weddell-Scotia Confluence

Yu. V. Artamonov, E. A. Skripaleva *, N. V. Nikolskii

Marine Hydrophysical Institute of RAS, Sevastopol, Russia
* *e-mail: sea-ant@yandex.ru*

Abstract
Based on the ECMWF ORA-S5 reanalysis data for 1958–2023, the paper analyses the average long-term structure of waters in the Weddell–Scotia Confluence and the climatic variability of its boundary characteristics. It is shown that this zone was most clearly manifested between Shishkov Island and the South Orkney Shelf. The northern boundary of this zone (Scotia Sea Front) was located above the southern slope of the South Scotia Ridge, and the southern boundary (Weddell Sea Front) was south of the Phillip Ridge. Both fronts were most intense in the 150–500 m layer. Near the South Orkney Shelf, the width of the Weddell–Scotia Confluence zone decreased by more than five times. The intensity of the fronts also weakened in the easterly direction, and they were mostly not traced east of the South Orkney Islands. On an interannual scale, the displacements of the Scotia Sea Front and the Weddell Sea Front in latitude did not exceed 0.5 degrees, while their intensity changed synchronously. From 1983 to 2010, a decrease in their intensity was observed, whereas from 1958 to 1982 and after 2010 there was an increase. In the time series of annual mean anomalies of temperature gradient values characterizing interannual changes in the intensity of the Scotia Sea Front and the Weddell Sea Front, a periodicity of 4 and 6 years was revealed. A significant positive correlation was found between the Antarctic Oscillation index and the interannual intensity anomalies of the fronts, with a phase lag of 0–3 years for the Weddell Sea Front and 3–5 years for the Scotia Sea Front. The tendency to increase the intensity of the Weddell–Scotia Confluence boundaries with an increase of the Antarctic Oscillation index values was especially clear over the past 10 years. During this period the high positive values of this index and maximum positive values of the Weddell Sea Front intensity anomalies were observed. Over the past 10 years, the Weddell–Scotia Confluence boundaries have strengthened markedly as the Antarctic Oscillation index increased. This period featured persistently high positive index values alongside maximum positive intensity anomalies in the Weddell Sea Front.

Keywords: Weddell Sea, Scotia Sea, potential sea water temperature, salinity, vertical water structure, water masses, thermohaline fronts, spatio-temporal variability, Antarctic Oscillation, South Oscillation

Acknowledgements: The work was carried out under FSBSI FRC MHI state assignment FNNN-2024-0014 “Fundamental studies of interaction processes in the ocean-atmosphere system forming the variability of the marine environment physical state on different spatio-temporal scales”.

For citation: Artamonov, Yu.V., Skripaleva, E.A. and Nikolskii, N.V., 2025. Climatic Variability of the Water Thermohaline Structure in the Weddell-Scotia Confluence. *Ecological Safety of Coastal and Shelf Zones of Se*a, (4), pp. 76–96.

Климатическая изменчивость термохалинной структуры вод в зоне слияния морей Уэдделла и Скоша

Ю. В. Артамонов, Е. А. Скрипалева *, Н. В. Никольский

Морской гидрофизический институт РАН, Севастополь, Россия
***** *e-mail: sea-ant@yandex.ru*

Аннотация
По данным реанализа *ECMWF ORA-S*5 за 1958–2023 гг. проанализирована среднемноголетняя структура вод в зоне слияния морей Уэдделла и Скоша и климатическая изменчивость характеристик ее границ. Показано, что эта зона наиболее четко выражена между о-вом Шишкова и Южно-Оркнейским шельфом. Ее северная граница (фронт моря Скоша) располагается над южным склоном хребта Южный Скоша, а южная (фронт моря Уэдделла) – южнее хребта Филипп. Оба фронта наиболее интенсивны в слое 150–500 м. В районе Южно-Оркнейского шельфа ширина зоны слияния уменьшается более чем в пять раз. Интенсивность фронтов также ослабевает в восточном направлении, восточнее Южно-Оркнейских о-вов они почти не прослеживаются. На межгодовом масштабе смещения фронта моря Скоша и фронта моря Уэдделла по широте не превышают 0.5°, при этом их интенсивность изменяется синхронно. С 1983 по 2010 г. наблюдалось понижение их интенсивности, с 1958 г. по 1982 г. и после 2010 г. – повышение. Во временны́х рядах среднегодовых аномалий значений градиентов температуры, характеризующих межгодовые изменения интенсивности фронта моря Скоша и фронта моря Уэдделла, выявлена периодичность в 4 и 6 лет. Между индексом Антарктического колебания и межгодовыми аномалиями интенсивности фронтов выявлена значимая положительная корреляция: для фронта моря Уэдделла – при фазовом сдвиге 0–3 года, для фронта моря Скоша – при фазовом сдвиге от 3 до 5 лет. Особенно четко тенденция к повышению интенсивности границ зоны слияния морей Уэдделла и Скоша при росте значений индекса Антарктического колебания проявилась в течение последних 10 лет. В этот период наблюдались высокие положительные значения этого индекса и максимальные положительные значения аномалий интенсивности фронта моря Уэдделла.

Ключевые слова: море Уэдделла, море Скоша, температура воды, соленость, вертикальная структура вод, водные массы, термохалинный фронт, пространственно-временная изменчивость, Антарктическое колебание, Южное колебание

Благодарности: работа выполнена в рамках темы государственного задания ФГБУН ФИЦ МГИ FNNN-2024-0014 «Фундаментальные исследования процессов взаимодействия в системе океан-атмосфера, формирующих изменчивость физического состояния морской среды на различных пространственно-временных масштабах».

Для цитирования: *Артамонов Ю. В., Скрипалева Е. А., Никольский Н. В.* Климатическая изменчивость термохалинной структуры вод в зоне слияния морей Уэдделла и Скоша // Экологическая безопасность прибрежной и шельфовой зон моря. 2025. № 4. С. 76–96. EDN XKZNOE.

Introduction

The Weddell-Scotia Confluence (WSC) is located in the southwestern part of the Atlantic Ocean Antarctic sector. It extends eastward from the South Shetland Islands along the South Scotia Ridge [1)]. This zone is one of the most biologically productive regions of the Southern Ocean, with high concentrations of phytoplankton and chlorophyll a in its waters. It is a key migration route for Antarctic krill, which travel eastward from their spawning grounds on the shelves of the Antarctic Peninsula [2)] [1–9]. The area's commercial importance has led to numerous publications analysing the features of the WSC thermohaline structure, which is a key abiotic factor influencing the spatial and temporal variability of water bioproductivity [3), 4), 5)] [10–21]. The vertical thermohaline structure of WSC waters differs qualitatively from that of the surrounding Antarctic-type waters. The Circumpolar Deep Water (CDW) layer, which is characterised by elevated temperature and salinity and is typical of Antarctic waters, undergoes noticeable transformation in the WSC. WSC waters are characterised by their own vertical structure with relatively weak stratification, and the subsurface layer down to a depth of 1000 m is almost homogeneous [1), 3), 5)] [10–18, 20]. According to [3)] [10, 12, 13], the causes of CDW transformation and the formation of a quasi-homogeneous layer with weak stratification can include winter vertical convection and subsidence of cold water observed during the warm season due to the melting of icebergs that accumulate on the South Scotia Ridge shelves. According to [17, 21], the WSC is characterized by subsidence of surface and subsurface waters, which leads to the formation of a water column with relatively low temperature and salinity. Moreover, according to [21], cold fresh shelf waters formed near the tip of the Antarctic Peninsula penetrate the WSC. These waters spread eastward along the northwestern periphery of the Weddell Sea Gyre, subsiding to intermediate depths due to their increased density resulting from the low temperature close to the ice melting point. This process results in cooling and freshening of the WSC waters. According to [19], the formation of the WSC water structure is influenced by convective mixing due to ice melting and by vertical currents within a system of numerous quasi-stationary topographic vortex formations characteristic of this area.

[1)] Gordon, A.L., 1967. Structure of Antarctic Water Between 20W and 170W. In: V. Bushnell, ed., 1967. *Antarctic Map Folio series. Folio 6*. American Geographical Society, 10 p.

[2)] Shulgovsky, K.E., 2005. [*Large-Scale Variability of Oceanological Conditions in the Western Part of the Atlantic Sector of the Antarctic and its Influence on the Distribution of Krill*]. Kaliningrad: AtlantNIRO, 148 p. (in Russian).

[3)] Chernyavsky, E.B., 1977. [*Frontal and Gradient Zones of the South Ocean*]. Moscow: Promyslovaya Okeanologiya. Iss. 6, 50 p. (in Russian).

[4)] Burkov, V.A., 1995. [Weddell-Scotia Confluence Zone]. In: IO RAS, 1995. [*Pelagic Ecosystems of the Atlantic Sector of Antarctica*]. Moscow: IO RAN, pp. 7–14 (in Russian).

[5)] Smith, S.G., 1989. *On the Weddell-Scotia Confluence and the Scotia Front:* Master's Thesis in Oceanography. Texas A&M University, 85 p. Available at: https:hdl.handle.net/1969.1/ETD-TAMU-1989-THESIS-S661 [Accessed: 24 November 2025].

According to existing concepts [3), 6)] [15, 18–20], the northern boundary of the WSC, which separates it from the waters of the southern Scotia Sea, is the Scotia Sea Front (SSF). The southern boundary, which separates the WSC from the waters of the northern Weddell Sea, is the Weddell Sea Front (WSF). In accordance with [15, 22–24], the SSF and WSF can be observed on the surface. Note that on the surface, they divide the modifications of the same body of water, the Antarctic Surface Water. At the same time, in the subsurface layer, they delineate the northern and southern limits of the transformed CDW layer [19, 20]. The SSF extends the continental water boundary east of Mordvinov (Elephant) Island and coincides with a relatively weak deep stream identified in the southern Scotia Sea, south of the Antarctic Circumpolar Current system [15, 22]. The branches of the WSF correspond to deep streams that form the north-western periphery of the Weddell Sea Gyre [15, 22, 24].

Most studies analysing the water structure of the WSC and the variability of its boundaries are based on data from contact measurements performed in different years and seasons on individual synoptic sections located relatively far from each other [5)] [10–13, 16, 18] or on outdated hydrological databases with low spatial and temporal coverage [17, 19, 20]. Due to high heterogeneity of contact measurement data and almost complete absence of information during the cold season, contradictions in the description of the WSC water structure persist to this day. Thus, according to [3)] [10], the temperature of the WSC waters is low from the surface to the bottom, whereas study [12] shows that a temperature maximum is observed at the surface of the WSC. It is claimed in [3)] [10–13] that the WSC surface salinity is elevated, while data from [3)] [10] show that high salinity is present at the bottom. Furthermore, the results of studies [13, 17] suggest that the salinity of the WSC waters is lower at depths of 200 m and below.

Based on archival climatic data from works [19, 20], the manifestations of the WSC boundaries (SSF and WSF) in the long-term average thermohaline fields were evaluated. The SSF is most clearly manifested in the temperature field at depths greater than 200 m and in the salinity field in the upper 250 m layer. The WSF is manifested deeper than 100 m in the temperature field and deeper than 300 m in the salinity field. These works also analysed the seasonal variability of the SSF. It was demonstrated that the front is located between 58° and 60° S at the surface throughout the year and reaches maximum intensity in March. However, due to the limited availability of hydrological data in the Weddell Sea and their complete absence in winter, the seasonal variations of the WSF could not be evaluated [19, 20].

Some studies have analysed the features of the water structure in the WSC area based on relatively short series of drifter and satellite measurements [4, 14, 15, 21, 23]. Higher spatio-temporal resolution satellite temperature measurements allowed the SSF to be detected in the sea surface temperature (SST) field and the features

---

[6)] Bogdanov, M.A., Oradovsky, S.G., Solyankin, E.V. and Khvatsky, N.V., 1969. [On the Frontal Zone of the Scotia Sea]. *Okeanologiya*, 9(6), pp. 966–974 (in Russian).

of the average long-term seasonal and interannual variability of this front's characteristics to be refined [23]. Using AVHRR Ocean Pathfinder data from JPL NOAA/NASA for the period 1985–2001, it was demonstrated that during the climatic seasonal cycle, an increase in SSF intensity at the surface was observed during the warm season. Meanwhile, interannual variations in the characteristics of the front manifest as changes in its intensity and latitudinal displacement. A significant relationship was identified between interannual anomalies in the characteristics of the front and anomalies in the areas of warm tropical waters in the Pacific Ocean caused by El Niño events. At the same time, the characteristics of the front responded weakly to changes in the Southern Oscillation index [23].

In recent years, high-resolution hydrological datasets have emerged that assimilate continuously updated SST data from contact and satellite measurements, optimally interpolated onto regular grids (e.g. NOAA OISST). This has enabled features in the climatic structure and seasonal variability of the WSF at the ocean surface to be refined [24]. It has been demonstrated that, to the west of the South Orkney Islands, the WSF is characterised by two branches in the average long-term SST field, intensifying during the summer period of the Southern Hemisphere (February–April) [24]. However, the structure and climatic variability of the SSF and WSF in the ocean subsurface layers, which form the boundaries of the WSC, remain largely unexplored.

The study aims to refine the characteristics of WSC manifestations in average long-term thermohaline fields, based on modern oceanic reanalysis data (ECMWF ORA-S5 курсив наверное не нужен), to analyse the climatic variability of SSF and WSF boundaries as well as to evaluate the influence of large-scale atmospheric circulation modes (Southern Annular Mode and Southern Oscillation) on interannual front characteristics.

Materials and methods

The study considers the region of the Southern Ocean located east of Mordvinov (Elephant) Island, between 55° and 40°W, and 59° and 62.5°S (Fig. 1, *a*, *b*). To construct the bottom relief scheme, data from General Bathymetric Chart of the Oceans (GEBCO) [7)] with a spatial resolution of 15″ were used. Monthly mean values of potential temperature (θ, °C) and salinity *S* (PSU), as well as zonal *U* and meridional *V* components of current velocities $\vec{V}$ (m/s), were utilised for each year from 1958 to 2023. These data were obtained from the reanalysis of the European Centre for Medium-Range Weather Forecasts OCEAN5 system (ECMWF ORAS5) [27]. They were interpolated onto grid nodes with a resolution of approximately 1/4° in longitude and 1/8° in latitude, distributed across 75 vertical levels in σ coordinates ranging from 0.5 to 5500 m [8)]. The reanalysis used the ocean model Nucleus for European Modelling of the Ocean (NEMO) and the ocean assimilation system NEMOVAR, which incorporates surface and subsurface temperature, salinity, sea ice concentration and sea level anomalies [25].

[7)] GEBCO. *Gridded Bathymetry Data*. [online] Available at: http://www.gebco.net/data_and_products/gridded_bathymetry_data/ [Accessed: 24 November 2025].

[8)] Copernicus Climate Change Service, Climate Data Store. 2021. *ORAS5 Global Ocean Reanalysis Monthly Data from 1958 to Present*. https://doi.org/10.24381/cds.67e8eeb7

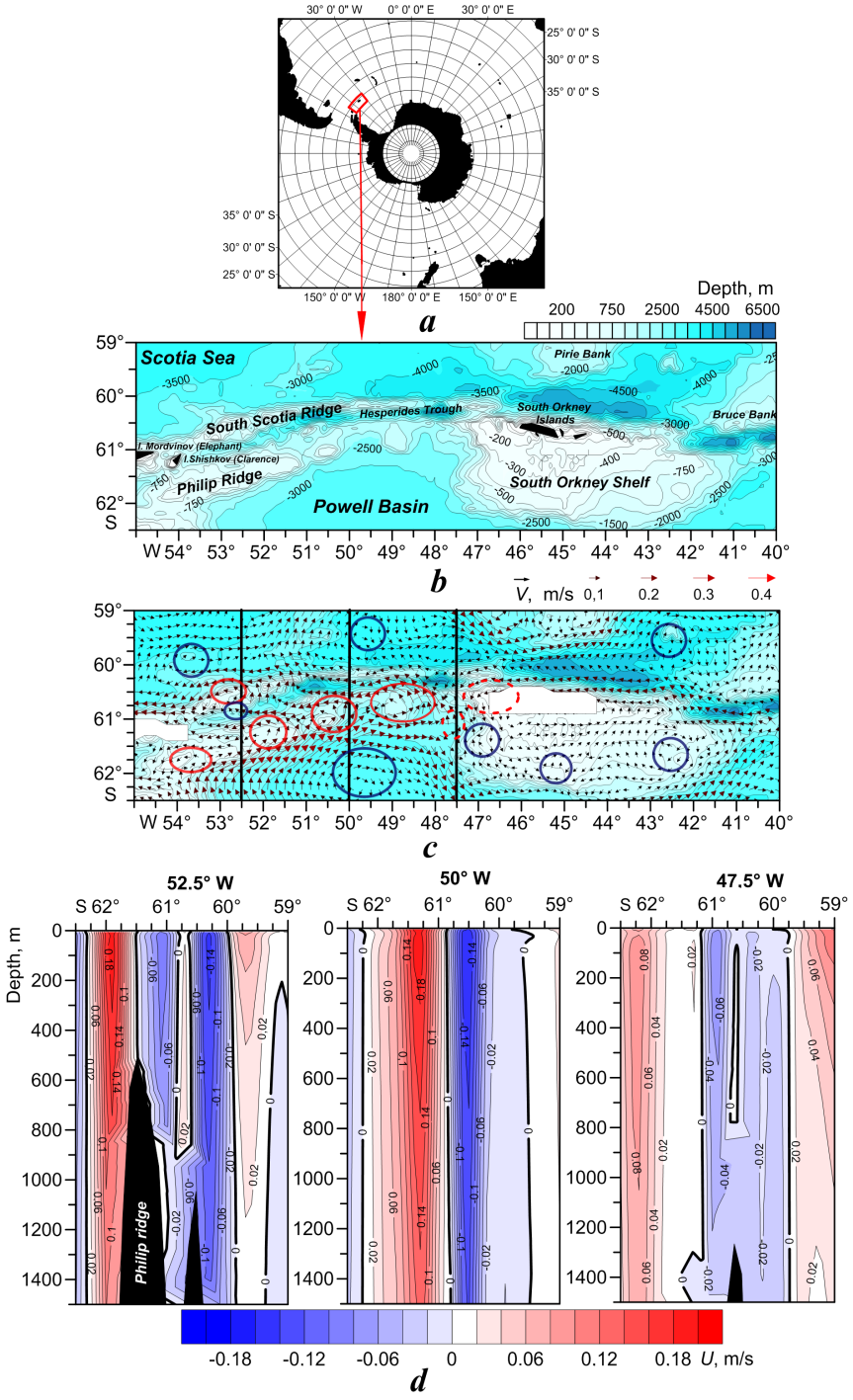

Fig. 1. Study area on the map of the South Ocean (*a*); bottom relief map of the area (*b*); distribution of current vectors at a depth of 200 m: the red ellipses denote anticyclonic gyres, the blue ellipses are cyclonic ones (*c*); vertical distributions of *U* values along 52.5°, 50° and 47.5°W (*d*)

Based on the source data, the average long-term and monthly climatic mean values of θ, S, the velocity modulus $\bar{V}$ and the direction of current vectors were calculated (Fig. 1, *c*). According to [9], the time series of the data used is sufficient for determining statistically reliable climatic norms.

The boundaries of the WSC (SSF and WSF) were determined by locating the extremes of the meridional temperature gradients (MTG) and meridional salinity gradients (MSG) on sections spaced 0.25° apart along meridians. Positive (negative) MTG and MSG values indicate an increase (decrease) in temperature and salinity values in the southern direction.

The interannual variability of the WSC boundaries was analysed in the temperature field, because this parameter largely determines the course of large-scale processes in the ocean–atmosphere system, serving as an indicator of the heat content of the active ocean layer [26, 27]. For this purpose, anomalies of the annual mean values of MTG extremes (AnMTG), which characterise the SSF and WSF, were calculated for each year relative to their average long-term values over the entire analysed period of 66 years. When calculating the anomalies, the absolute values of the MTG extremes were used. To assess the connections between the variability of atmospheric circulation and interannual variations in the intensity of the SSF and WSF, cross-correlation functions with a 95% statistical significance level ($\alpha = 0.05$) were analysed between the time series of annual mean AnMTG values and the indices of the Southern Oscillation (SO) and Antarctic Oscillation (AAO), which characterise the Southern Annular Mode [1, 28, 29]. When calculating the cross-correlation functions between the AnMTG values and the AAO index, the AnMTG time series from 1979 to 2023 were used, corresponding to the period for which AAO index data is available. SO and AAO index values were obtained from the National Oceanic and Atmospheric Administration (NOAA) website [10), 11)].

Results and discussion

Figs. 2–4 show examples of the vertical distribution of the long-term mean temperature and salinity values and their meridional gradients. Analysis of these distributions revealed no clear signs of the WSC (the absence of sharp thermohaline extremes in the vertical structure due to the subsidence of colder, fresher waters) in the climatic fields of the upper 100–150 m layer, which is consistent with earlier studies [1), 3), 5)] [10–21]. The upper 100–150 m layer has the typical vertical structure of the Antarctic zone characterised by a well-defined subsurface layer of Antarctic Winter Water (AWW) with a minimum temperature and relatively low salinity.

---

9) Monin, A.S., 1999. [*Hydrodynamics of the Ocean Atmosphere and Earth's Interior*]. Saint Petersburg: Gidrometeoizdat, 523 p. (in Russian).

10) Climate Prediction Center. *The Southern Oscillation Index (SOI).* 2025. [online] Available at: https://www.cpc.ncep.noaa.gov/products/analysis_monitoring/ensocycle/soi.shtml [Accessed: 24 November 2025].

11) Climate Prediction Center. *Antarctic Oscillation (AAO).* 2025. [online] Available at: https://www.cpc.ncep.noaa.gov/products/precip/CWlink/daily_ao_index/aao/aao.shtml [Accessed: 24 November 2025].

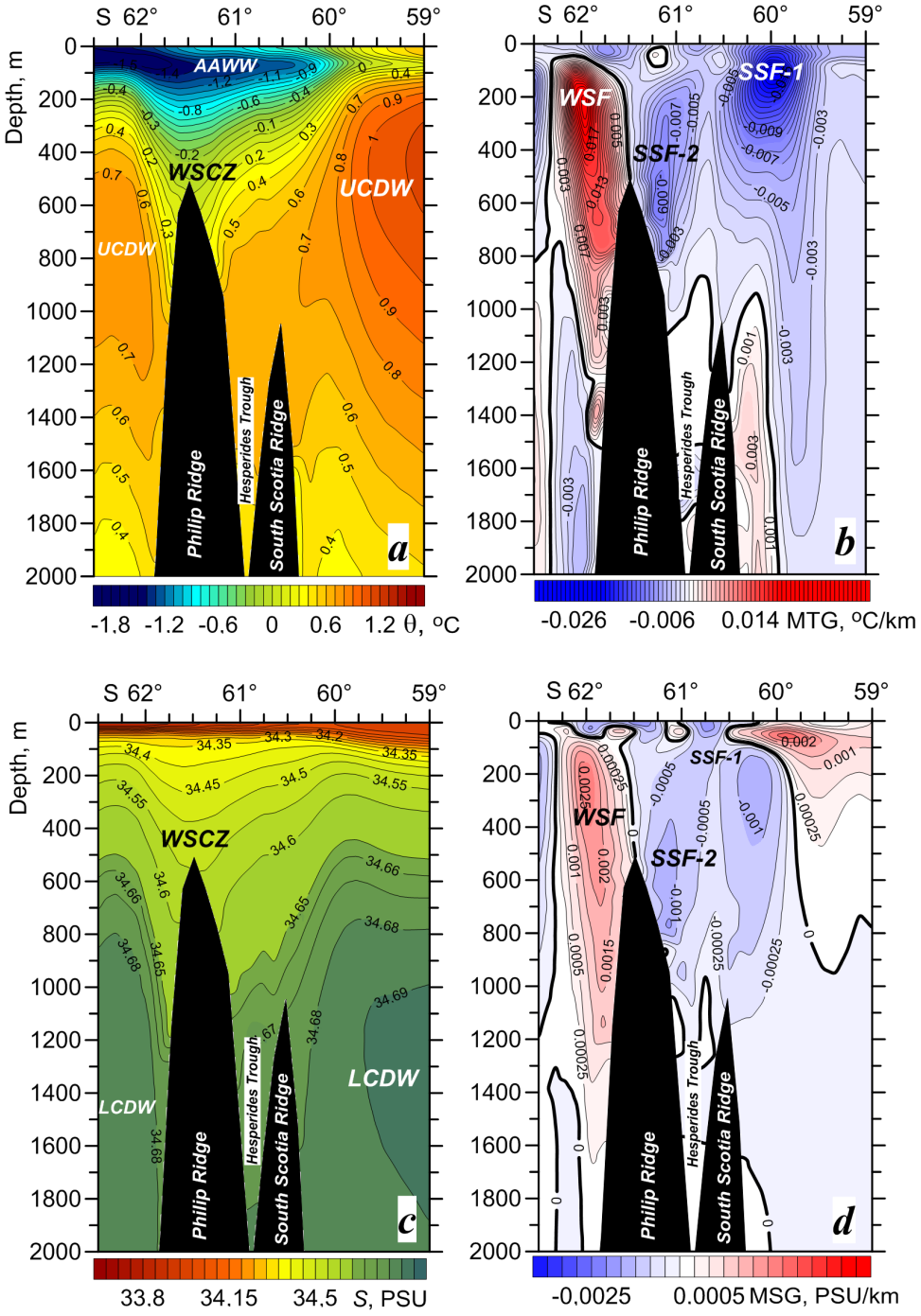

Fig. 2. Vertical distributions of annual mean values of temperature (*a*), meridional temperature gradients (MTG) (*b*), salinity (*c*), meridional salinity gradients (MSG) (*d*) along 52.5°W

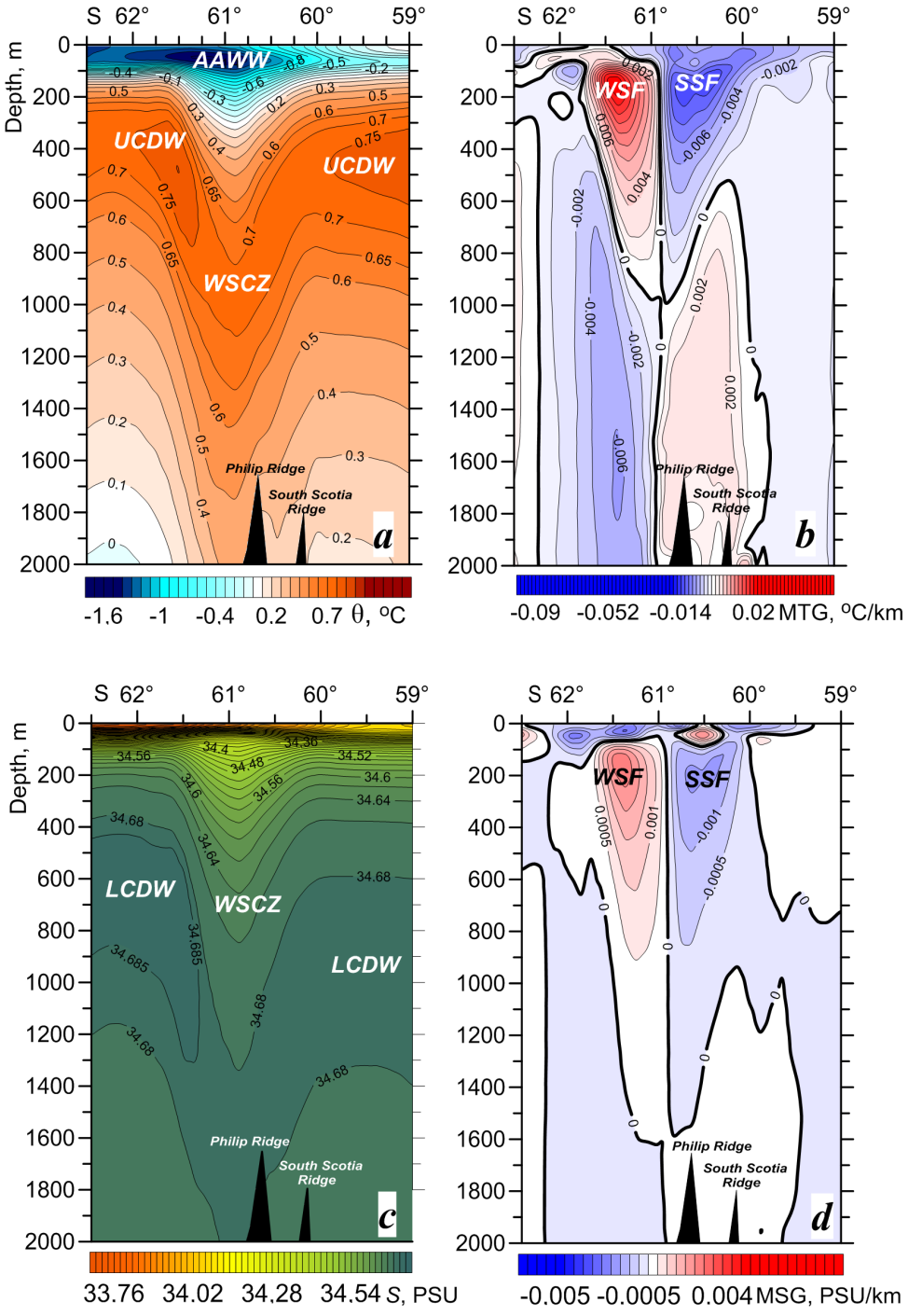

Fig. 3. Vertical distributions of annual mean values of temperature (*a*), MTG (*b*), salinity (*c*), MSG (*d*) along 50°W

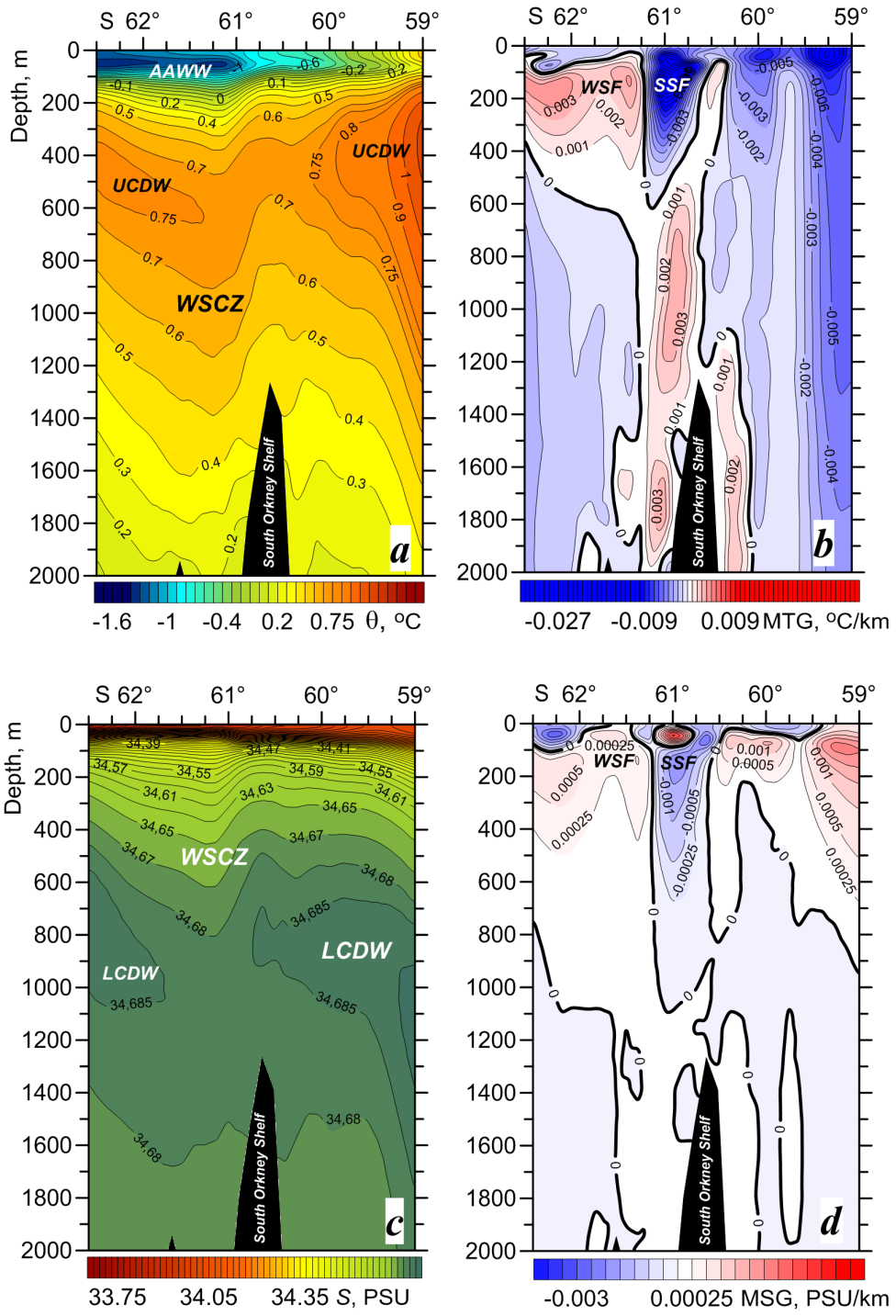

Fig. 4. Vertical distributions of annual mean values of temperature (*a*), MTG (*b*), salinity (*c*), MSG (*d*) along 47.5°W

The subsidence of colder, less saline water, which is characteristic of the WSC, is clearly evident in the long-term average thermohaline fields below the AWW layer. This disrupts the CDW layer (Figs. 2, *a*, *c*; 3, *a*, *c*; 4, *a*, *c*).

The transformation of the vertical water structure in the WSC is reflected in the θ and S curves (Fig. 5). The waters of the Scotia Sea to the north and the Weddell Sea (Powell Basin) to the south of the WSC are characterised by well-defined extremes corresponding to the AWW and CDW cores. In the WSC area, however, only the AWW core manifests as an extremum, below which a quasi-homogeneous layer is evident, with no clearly expressed extremum corresponding to the CDW (Fig. 5).

The waters of the WSC are characterised by weak temperature and salinity gradients. The northern boundary (SSF) has maximum negative MTG and MSG values, while the southern boundary (WSF) has maximum positive MTG and MSG values (Figs. 2, *b*, *d*; 3, *b*, *d*; 4, *b*, *d*).

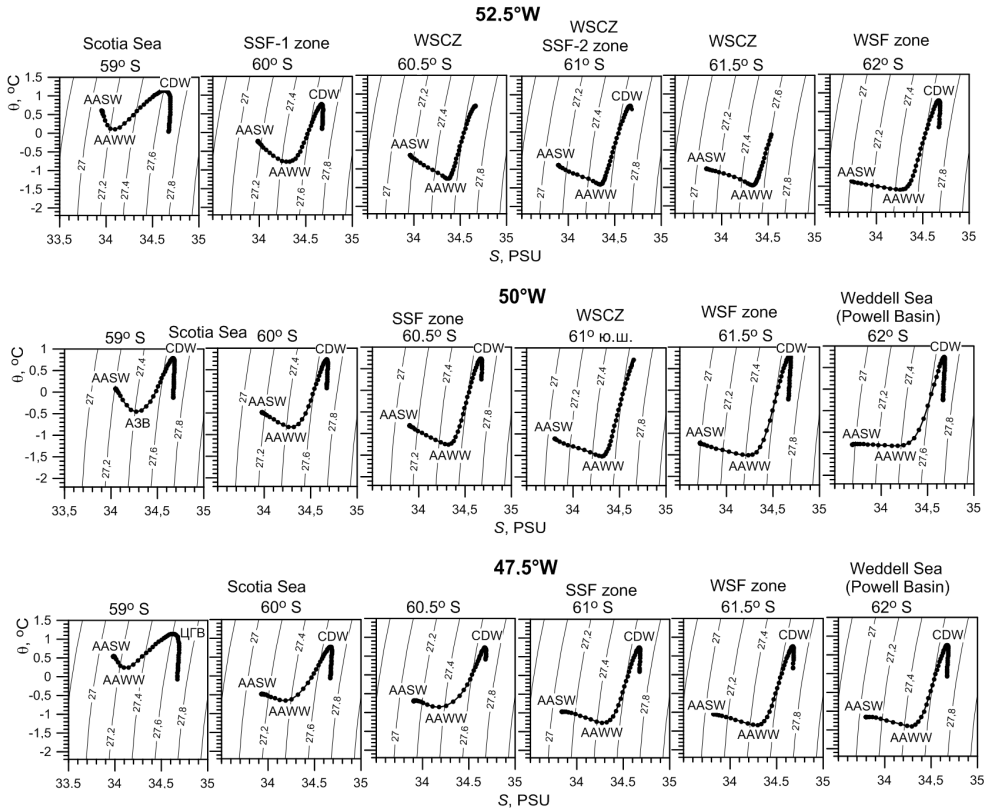

Fig. 5. Annual averaged θ,*S*-curves at different grid nodes on the meridians 52.5°W, 50°W and 47.5°W

While the general features of the WSC are preserved (subsidence of cold, low-salinity waters, and high MTG and MSG values at its boundaries), the position of its boundaries and the depth of water subsidence in different areas of the body of water differ. This is related to the features of water circulation caused by the bottom relief. Current vector distribution at a depth of 200 m revealed a significant presence of anticyclonic vortices and meanders over the South Scotia and Phillip Ridges, and cyclonic vortices in the Scotia Sea, the Hesperides Trough, the Powell Basin and the southern part of the South Orkney Shelf (Fig. 1, *b*, *c*). The vertical distribution of the zonal velocity component U clearly shows oppositely directed flows, which correspond to the northern and southern peripheries of these vortex formations and extend to depths of 900–1500 m (Fig. 1, *d*).

Analysis of the vertical distribution of temperature, salinity, MTG and MSG revealed that the WSC was most pronounced to the east of Mordvinov (Elephant) Island. Here, subsidence of the waters occurs over the South Scotia and Phillip Ridges. At 52.5°W, the WSC extends almost to the bottom over the Phillip Ridge, completely disrupting the CDW layer and the cores of its upper (UCDW) and lower (LCDW) modifications (Fig. 2, *a*, *c*). Within the latitudinal limits of the WSC over the deep-water Hesperides Trough, a slight rise in isotherms and isohalines is evident, which is associated with the topographic cyclonic meander observed in this area (Fig. 1, *c*, *d*). Consequently, the northern boundary of the WSC in the thermohaline fields exhibits a bimodal structure. One branch of the SSF is located approximately at 60°S (over the South Scotia Ridge) and is most developed in the 100–400 m layer. The second branch of the SSF is located north of the Phillip Ridge, approximately at 61°S, and is most developed in the 200–800 m layer (Fig. 2, *b*, *d*). The distributions of the annual mean MTG and MSG at the 200 m horizon along 52.5°W show two branches of the SSF (SSF-1 and SSF-2) in the temperature and salinity fields (Fig. 6). The southern boundary of the WSC (WSF) is located south of Phillip Ridge at 62°S, where it is most intense in the 100–700 m layer (Figs. 2, *b*, *d*; 6).

In the central part of the water area (50° W), colder, less saline waters descend over the Phillip Ridge spur in an anticyclonic meander area (Fig. 1, *c*) to depths of approximately 1000 m in the temperature field and 1500 m in the salinity field. This results in a significant transformation and deepening of the CDW layer as well as the disruption of the UCDW and LCDW cores (Fig. 3, *a*, *c*). The SSF is clearly visible in the temperature and salinity fields at approximately 60.5–60.75°S over the southern slope of the South Scotia Ridge, while the WSF is visible at the northern boundary of the Powell Basin at 61.375°S (Fig. 6). Both fronts are most intense in the 100–600 m layer (Fig. 3, *b*, *d*).

Further east, at the western boundary of the South Orkney Shelf (47.5°W), the main subsidence of waters also occurs in the area characterised by an anticyclonic meander (Fig. 4, *a*, *c*). The intensity and vertical extent of the SSF and WSF decrease; both fronts are most developed in the 100–400 m layer. The SSF is located at approximately 60.85–61°S and the WSF at approximately 61.375°S (Fig. 4, *b*, *d*; 6).

Overall, closer to the South Orkney Shelf, the width of the WSC and the intensity of its boundaries decrease noticeably (Fig. 6). At a depth of 200 m, the intensity of the SSF decreases from 0.02 °C/km in the western part of the WSC to 0.01 °C/km at the western boundary of the South Orkney Shelf while the intensity of the WSF decreases from 0.025 to 0.005 °C/km (Fig. 6, *a*).

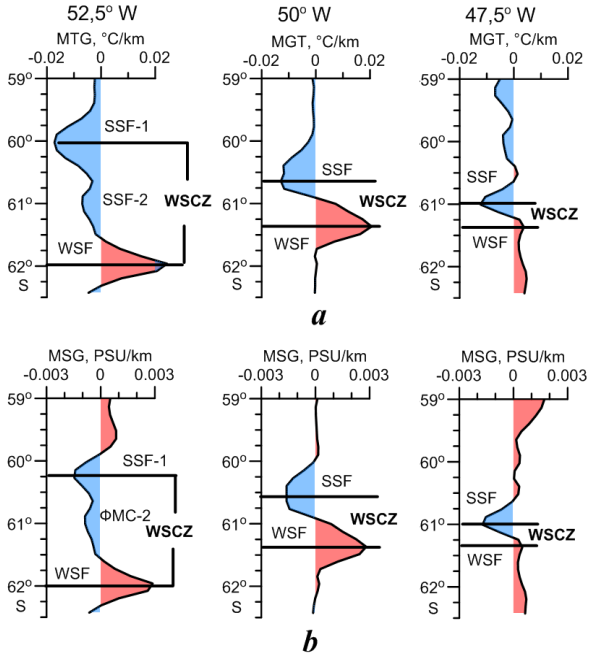

Fig. 6. Distributions of annual averaged MTG (*a*) and MSG (*b*) and the position of the Weddell–Scotia Confluence boundaries (Scotia Sea Front (SSF) and Weddell Sea Front (WSF)) at a depth of 200 m along the 52.5°W, 50°W and 47.5°W

In the salinity field, the intensity of the SSF remains relatively consistent across the landscape, whereas the intensity of the WSF decreases from west to east, dropping from 0.003 to 0.001 PSU/km (Fig. 6, *b*). In the thermohaline fields, the width of the WSC (the distance between the SSF and WSF axes) decreases from west to east, dropping from approximately 223 km (2° latitude) at 52.5°W to 42 km (0.375° latitude) at 47.5°W (Fig. 6). East of the South Orkney Islands, the WSC does not manifest in the annual mean climatic thermohaline fields, and the Scotia Sea and Weddell Sea fronts are almost indistinguishable.

Thus, examining distributions of thermohaline characteristics on vertical sections showed that the WSC was not clearly expressed in the climatic fields in the upper layer occupied by the Antarctic surface and Antarctic winter water masses. The horizontal distributions of temperature and salinity in the WSC area at the surface (Fig. 7, *a*, *b*) and below the AWW layer (Fig. 7, *c*, *d*) differ considerably. Within the latitudinal limits of the WSC at the surface, a decrease in temperature and salinity is observed in the southern direction, with a fall of 0 to −1 °C and 33.95 to 33.8 PSU, respectively (Fig. 7, *a*, *b*). Between approximately 49.5° and 47.5°W, the quasi-zonality of isohalines in the WSC area is noticeably disrupted.

Here, an elongated tongue of lower-salinity waters is present in the northwestern direction (Fig. 7, *b*). In this area temperature field, a slight shift of isotherms to the north is also observed (Fig. 7, *a*). Analysis of the distribution of current vectors in the upper 100 m layer revealed a large-scale anticyclonic meander, along the eastern edge of which waters with reduced temperature and salinity from the Powell Basin enter the WSC via the deep-water passage to the west of the South Orkney Shelf (Fig. 1, *b*). The surface distributions of temperature and salinity (the absence of temperature extremes and a salinity decrease in the central part of the WSC) refine the results of previous studies which claim an increase in salinity in the surface layer of waters in the WSC [10, 13], as well as extreme temperature values (maximum [12] or minimum [3)] [10]).

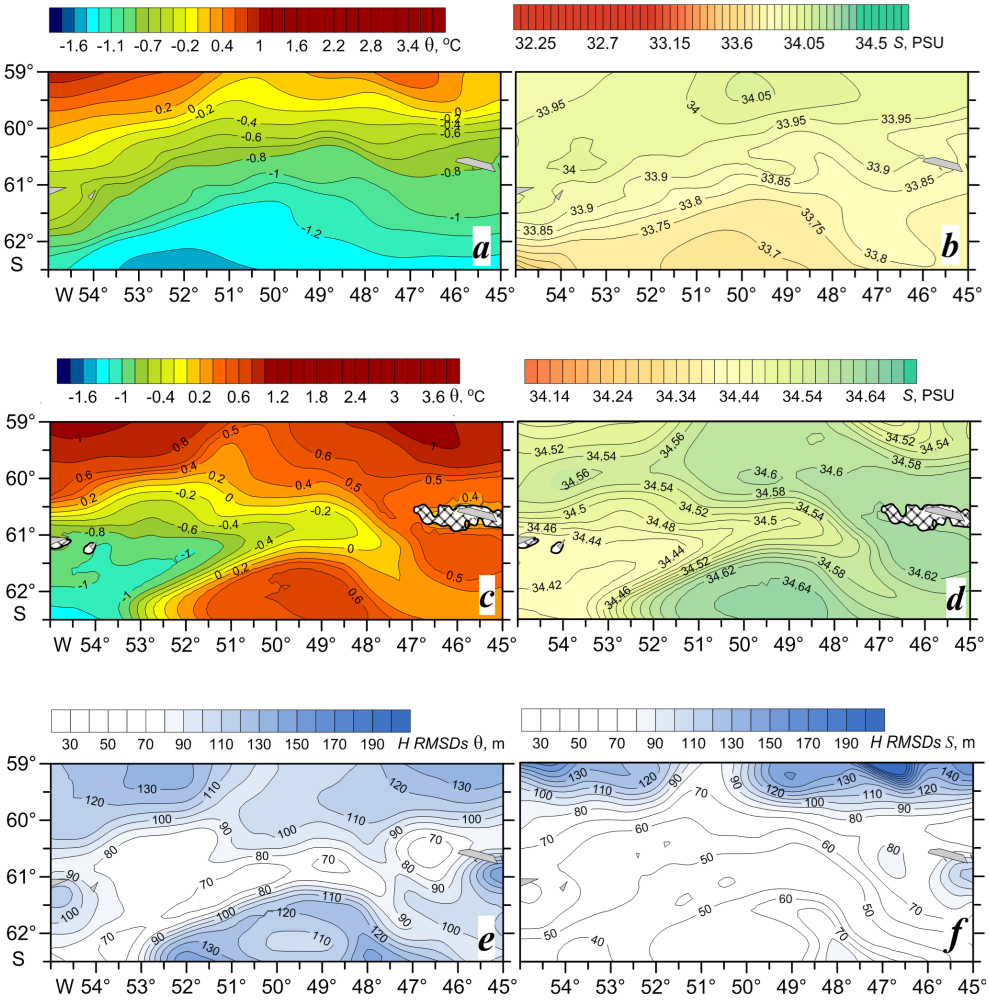

F i g . 7. Distributions of annual mean values of temperature (*a*, *c*) and salinity (*b*, *d*) at the surface (*a*, *b*) and at a depth of 200 m (*c*, *d*), depth of the seasonal signal penetration in the temperature (*e*) and salinity (*f*) fields

In contrast to the surface, the temperature and salinity distribution maps below the AWW layer at a depth of 200 m (рис. 7, *c*, *d*) reveal a distinct tongue of cooler, less salty water. This tongue extends along Phillip Ridge toward the South Orkney Shelf to the east. Clustering of isotherms and isohalines is observed at the boundaries of this tongue, which characterises the manifestation of the WSC boundaries. The configuration of the tongue of waters with reduced temperature and salinity, as well as the current vectors at the 200 m horizon (Fig. 1, *c*), indicate the penetration of colder and less saline shelf waters into the WSC area from the Powell Basin. These waters are formed over the shallow shelf of the Antarctic Peninsula. This finding is consistent with the results of the study [21].

When assessing the climatic variability of the WSC boundary characteristics (SSF and WSF), the depth of penetration of the seasonal signal (H SDseason) in the thermohaline fields was analysed. This depth was conventionally defined as the point at which the intra-annual standard deviation of temperature and salinity decreased by an order of magnitude (see Fig. 7, *e*, *f*). Within the WSC, the H SDseason values did not exceed 70–90 m in the temperature field and 50–80 m in the salinity field (Fig. 7, *e*, *f*). In other words, the layer of transformed CDW in the WSC area is almost unaffected by seasonal changes. Since seasonal fluctuations in the thermohaline fields do not penetrate to the upper depth at which the SSF and WSF manifest (100–150 m), the climatic variability of the WSC boundaries was analysed on the interannual scale using the annual mean values of the front characteristics.

Despite significant progress in creating and improving modern reanalyses, their quality for Antarctica remains low due to a key limitation: the extremely small amount of source data available for model assimilation. In the subsurface layers, where there is significantly less source data than at the surface, any interannual trends obtained should be considered estimates.

Some features of the interannual variability of the characteristics of the SSF and WSF in the subsurface layer, which is deeper than the AWW, can be explained by physical and geographical factors, as identified through the reanalysis data used. Thus, analysing the time series of the latitudinal positions of the MTG extremes that characterise the SSF and WSF in the temperature field revealed that, on the interannual scale from 1958 to 2023, the latitudinal displacement of the fronts does not exceed 0.5°. At the same time, the stable position of the WSC boundaries is determined by the features of the bottom relief. For instance, at the 50° W meridian, which passes through the centre of the WSC, the SSF is located over the southern slope of the South Scotia Ridge within the latitudinal band 60.25–60.75° S (Fig. 8, *a*) throughout all 66 years, while the WSF is situated south of Phillip Ridge at the northern boundary of the Powell Basin within the latitudinal band 61.25–61.75° S (Fig. 8, *c*).

The distribution of annual mean MTG extremes (AnMTG) anomalies corresponding to the SSF and WSF showed that these fronts intensified and weakened in synchrony on the interannual scale (Fig. 8, *a*, *c*). From 1983 to 2010, a general decrease in the intensity of the SSF and WSF was observed, with both fronts being significantly weakened from 1987 to 1990. During this period, the width of the WSC increased by almost one degree due to maximum displacement of the SSF

northward to 60.25°S and the WSF southward to 61.75°S. From 1958 to 1982 and after 2010, the intensity of the SSF and WSF increased. During periods of significant change in the intensity of the WSC boundaries, the southern boundary exhibited the greatest change, with extreme interannual variations in WSF intensity noticeably exceeding those in SSF intensity. The maximum positive values of AnMTG are 0.008 °C/km for the SSF and 0.012 °C/km for the WSF. The maximum negative values of AnMTG for the SSF are −0.01 °C/km and for the WSF they are −0.25 °C/km (Fig. 8, *a*, *c*).

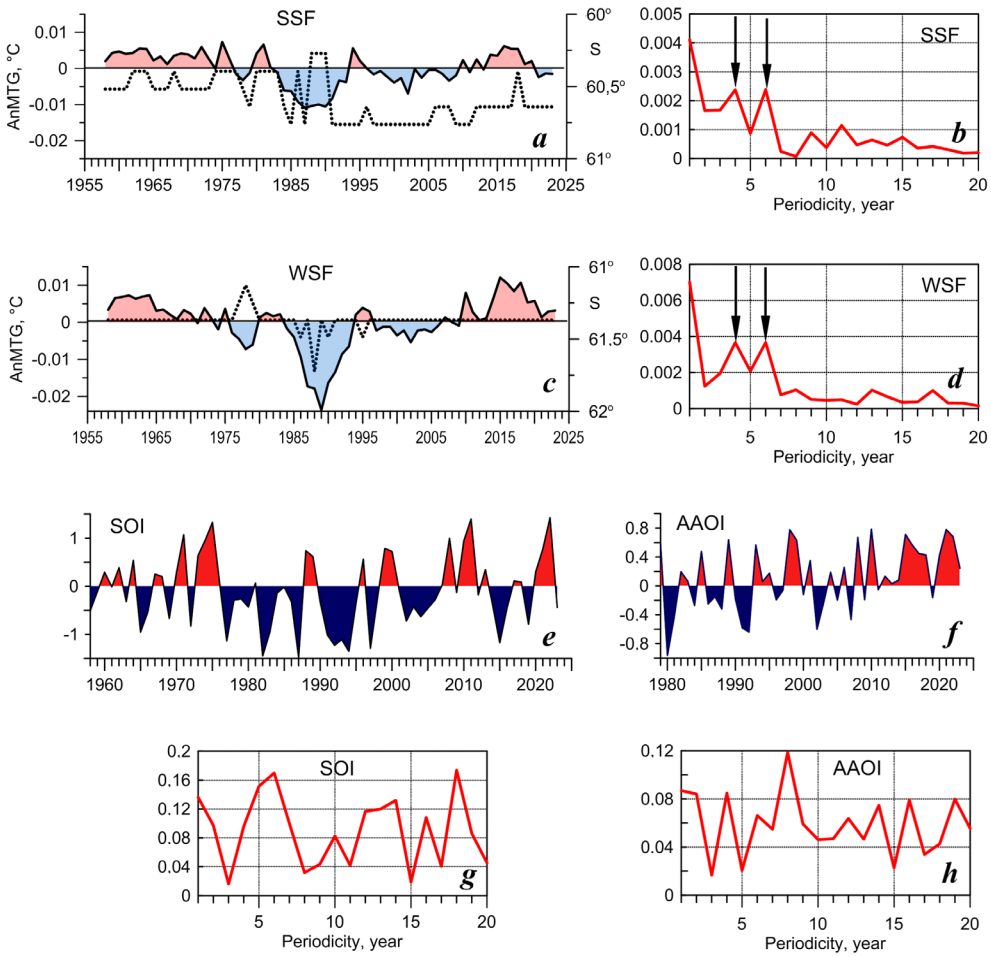

Fig. 8. Interannual variability of MTG annual mean anomalies and latitudinal position (black dotted line) of the SSF (*a*) and WSF (*c*), spectra of AnMTG time series of the SSF (*b*) and WSF (*d*) at a depth of 200 m at 50°W, distributions of annual mean values of the South Oscillation (SO) (*e*) and Antarctic Oscillation (AAO) (*f*) indices and their spectra (*g*, *h*)

No significant trends characterising the general tendencies of long-period variability in the intensity of the SSF and WSF were identified in the time series of annual mean AnMTG. The spectra of the AnMTG time series revealed periodicities of four and six years in the interannual changes in the intensity of the SSF and WSF (Fig. 8, *b, d*), similar to the variability periods of the Southern Oscillation (SO) and Antarctic Oscillation (AAO) indices (Fig. 8, *e–h*). Features similar to those observed in the interannual variability of the WSC boundaries (absence of a significant trend in the interannual anomaly time series and periodic alternation of positive and negative anomalies every 2–5 years) were also observed in the sea surface temperature field in the Atlantic sector of Antarctica [30].

Analysis of the cross-correlation functions revealed no significant relationship between the interannual changes in the SSF and WSF intensity anomalies and the changes in the SOI. A significant positive correlation was noted between the intensity of the WSF and the AAO index, with a maximum value of $R \sim 0.4$ at zero phase shift at a depth of 100 m (Fig. 9, *a*) and at a shift of 3 years at a depth of 200 m (Fig. 9, *b*).

A significant positive relationship is also observed between the SSF intensity and the AAO index, with a maximum value of $R \sim 0.35$ at a phase shift of 5 years at a depth of 100 m (Fig. 9, *a*) and at a phase shift of 3–5 years at a depth of 200 m (Fig. 9, *b*). Thus, an increase (decrease) in AAO index values tends to be accompanied by an increase (decrease) in WSC boundary intensity. This tendency has been particularly evident over the last 10 years, when high positive values of the AAO index (except in 2019) and maximum positive values of the WSC intensity anomalies have been observed. As oceanic fronts act as “mixing barriers” [1, 4, 31], strengthening the frontal boundaries of the WSC hinders the exchange of water between the WSC and the Scotia and Weddell Seas. This contributes to the concentration of biogenic elements and krill juveniles within the WSC, increasing the bioproductivity of its waters. One possible cause of the strengthening of the fronts that limit the WSC, as the AAO index values increase, may be the intensification of eastward transport in the atmospheric boundary layer and the zonal component of wind stress. At the same time, the band of intense westerly winds shifts southwards towards the WSC, reaching approximately 60°S [29, 32–34].

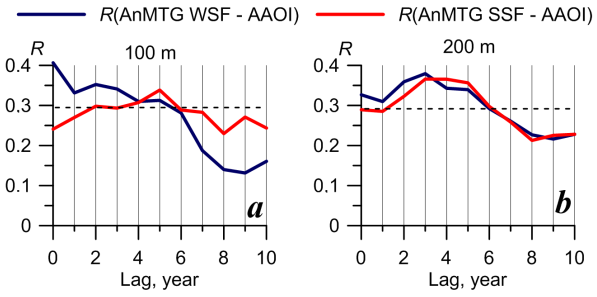

Fig. 9. Cross-correlation functions between the annual averaged values of the MTG anomalies of the SSF and WSF and the Arctic Oscillation index values at depths of 100 m (*a*) and 200 m (*b*). Dashed lines are the boundaries of the confidence interval of the 95% level of statistical significance ($\alpha = 0.05$)

Conclusion

Based on ECMWF ORA-S5 reanalysis data from 1958 to 2023, the characteristics of WSC manifestation in average long-term thermohaline fields have been refined. The WSC is most clearly manifested between Shishkov (Clarence) Island and the western boundary of the South Orkney Shelf. Below the AWW layer here, subsidence of colder, less saline water is observed, accompanied by transformation of the CDW layer and disruption to the cores of its upper and lower modifications. The northern boundary of the WSC (the Scotia Sea Front) is found to be situated over the southern slope of the South Scotia Ridge, while the southern boundary (the Weddell Sea Front) is found to pass south of the Phillip Ridge at the northern boundary of the Powell Basin. Both fronts are most intense in the 150–500 m layer. Closer to the South Orkney Shelf, the width of the WSC decreases by more than fivefold (from 2° to 0.375° of latitude). The intensity of the SSF and WSF decreases towards the east, and east of the South Orkney Islands, these fronts become indistinct.

On the interannual scale it is shown that the latitudinal displacements of the WSC boundaries do not exceed 0.5°, while their stable latitudinal position is determined by the bottom relief features. Throughout the entire analysed period, the SSF is located over the southern slope of the South Scotia Ridge in the central part of the WSC, between 60.25° and 60.75°S, while the WSF is located south of the Phillip Ridge, between 61.25° and 61.75°S.

It is established that the boundaries of the WSC both intensify and weaken in synchrony on the interannual scale. From 1983 to 2010, a decrease in the intensity of the SSF and WSF was observed, and both fronts were at their weakest from 1987 to 1990. The intensity of the SSF and WSF increased from 1958 to 1982 and after 2010. During periods of significant intensification or weakening of the WSC boundaries, the intensity anomalies of the WSF exceed those of the SSF by 1.5–2.5 times.

No significant trends characterising the general tendencies of long-period variability in the intensity of the SSF and WSF temperature gradient values were identified in the time series of annual mean anomalies. However, periodicities of four and six years were detected, which are close to the periodicities of the Southern Oscillation and the Southern Annular Mode. A significant positive correlation ($R \sim 0.4$) was identified between the intensity anomalies of the WSF and the AAO index at zero phase shift at a depth of 100 m, and at a shift of three years at a depth of 200 m. A significant positive relationship ($R \sim 0.35$) is also observed between the intensity anomalies of the SSF and the AAO index at a phase shift of 5 years at a depth of 100 m, and at a phase shift of 3–5 years at a depth of 200 m. This tendency for the WSF boundaries to increase in intensity with rising AAO index values has been particularly evident over the last 10 years, when high positive AAO index values and maximum positive WSF intensity anomaly values were observed. However, no significant relationship was identified between interannual changes in SSF and WSF intensity anomalies and changes in the SOI.

REFERENCES

1. Maslennikov, V.V., 2003. *Climatic Variability and Marine Ecosystem of the Antarctica*. Moscow: VNIRO Publishing, 295 p. (in Russian).
2. Zimin, A.V., 2005. The Monitoring of Dynamic Processes in the Scotia Sea and Forecast Opportunity of Commercial Fishery Conditions Using Satellite Altimetry Data. *Issledovanie Zemli iz Kosmosa*, 3, pp. 66–72 (in Russian).
3. Kahru, M., Mitchell, B.G., Gille, S.T., Hewes, C.D. and Holm-Hansen, O., 2007. Eddies Enhance Biological Production in the Weddell-Scotia Confluence of the Southern Ocean. *Geophysical Research Letters*, 34(14), L14603. https://doi.org/10.1029/2007GL030430
4. Venables, H., Meredith, M.P., Atkinson, A. and Ward, P., 2012. Fronts and Habitat Zones in the Scotia Sea. *Deep-Sea Research Part II: Topical Studies in Oceanography*, 59–60, pp. 14–24. https://doi.org/10.1016/j.dsr2.2011.08.012
5. Thompson, A.F. and Youngs, M.K., 2013. Surface Exchange Between the Weddell and Scotia Seas. *Geophysical Research Letters*, 40(22), pp. 5920–5925. https://doi.org/10.1002/2013GL058114
6. Arzhanova, N.V. and Artamonova, K.V., 2014. Hydrochemical Structure of Water Masses in Areas of the Antarctic Krill (*Euphausia superba Dana*) Fisheries. *Trudy VNIRO*, 152, pp. 118–132 (in Russian).
7. Siegel, V. and Watkins, J.L., 2016. Distribution, Biomass and Demography of Antarctic Krill, Euphausia superba. In: V. Siegel, ed., 2016. *Biology and Ecology of Antarctic Krill*. Advances in Polar Ecology, vol. 1. Cham: Springer, pp. 21–100. https://doi.org/10.1007/978-3-319-29279-3_2
8. Spiridonov, V.A., Zalota, A.K., Yakovenko, V.A. and Gorbatenko, K.M., 2020. Composition of Population and Transport of Juveniles of Antarctic Krill in Powell Basin Region (Northwestern Weddell Sea) in January 2020. *Trudy VNIRO*, 181, pp. 33–51. https://doi.org/10.36038/2307-3497-2020-181-33-51 (in Russian).
9. Morozov, E.G., Spiridonov, V.A., Molodtsova, T.N., Frey, D.I., Demidova, T.A. and Flint, M.V., 2020. Investigations of the Ecosystem in the Atlantic Sector of Antarctica (Cruise 79 of the R/V Akademik Mstislav Keldysh). *Oceanology*, 60(5), pp. 721–723. https://doi.org/10.1134/S0001437020050161
10. Deacon, G.E.R. and Moorey, J.A., 1975. The Boundary Regions Between Currents from the Weddell Sea and Drake Passage. *Deep Sea Research*, 22(4), pp. 265–268. https://doi.org/10.1016/0011-7471(75)90031-5
11. Deacon, G.E.R. and Foster, T.D., 1977. The Boundary Region Between the Weddell Sea and Drake Passage Currents. *Deep Sea Research*, 24(6), pp. 505–510. https://doi.org/10.1016/0146-6291(77)90525-2
12. Gordon, A.L., Georgi, D.T. and Taylor, H.M., 1977. Antarctic Polar Frontal Zone in Western Scotia Sea Summer 1975. *Journal of Physical Oceanography*, 7(3), pp. 309–328. https://doi.org/10.1175/1520-0485(1977)007<0309:APFZIT>2.0.CO;2
13. Patterson, S.L. and Sievers, H.A., 1980. The Weddell-Scotia Confluence. *Journal of Physical Oceanography*, 10(10), pp. 1584–1610. https://doi.org/10.1175/1520-0485(1980)010<1584:TWSC>2.0.CO;2
14. Muench, R.D., Gunn, J.T. and Husby, D.M., 1990. The Weddell-Scotia Confluence in Midwinter. *Journal of Geophysical Research: Oceans*, 95(C10), pp. 18177–18190. https://doi.org/10.1029/JC095iC10p18177
15. Peterson, R.G. and Stramma, L., 1991. Upper-Level Circulation in the South Atlantic Ocean. *Progress in Oceanography*, 26(1), pp. 1–73. https://doi.org/10.1016/0079-6611(91)90006-8

16. Whitworth, T., Nowlin, W.D., Orsi, A.H., Locarnini, R.A. and Smith, S.G., 1994. Weddell Sea Shelf Water in the Bransfield Strait and Weddell-Scotia Confluence. *Deep Sea Research*. *Part I: Oceanographic Research Papers*, 41(4), pp. 629–641. https://doi.org/10.1016/0967-0637(94)90046-9
17. Artamonov, Yu.V., 2002. Features of the Hydrological Structure of the Confluence Zone of the Weddell and Scotia Seas in the Summer of the Southern Hemisphere. In: MHI, 2002. *Monitoring Systems of Environment*. Sevastopol: MHI. Iss. 4, pp. 371–380. (in Russian).
18. Heywood, K.J., Naveira Garabato, A.C., Stevens, D.P. and Muench, R.D., 2004. On the Fate of the Antarctic Slope Front and the Origin of the Weddell Front. *Journal of Geophysical Research*, 109(C6), C06021. https://doi.org/10.1029/2003JC002053
19. Artamonov, Yu.V., Bulgakov, N.P., Lomakin, P.D. and Skripaleva, E.A., 2004. Vertical Thermohaline Structure, Water Masses, and Large-Scale Fronts in the Southwest Atlantic and Neighboring Antarctic Water Areas. *Physical Oceanography*, 14(3), pp. 161–172. https://doi.org/10.1023/B:POCE.0000048898.31072.cc
20. Lomakin, P.D. and Skripaleva, E.A., 2008. *Circulation and Waters Structure in Southwestern Part of Atlantic Ocean and Adjacent Areas of Antarctica.* Sevastopol: ECOSI-Gidrofizika, 116 p. (in Russian).
21. Meredith, M.P., Meijers, A.S., Naveira Garabato, A.C., Brown, P.J., Venables, H.J., Abrahamsen, E.P., Jullion, L. and Messias, M.-J., 2015. Circulation, Retention, and Mixing of Waters Within the Weddell-Scotia Confluence, Southern Ocean: The Role of Stratified Taylor Columns. *Journal of Geophysical Research: Oceans*, 120(1), pp. 547–562. https://doi.org/10.1002/2014JC010462
22. Artamonov, Yu.V., Skripaleva, E.A. and Nikolsky, N.V., 2022. Climatic Structure of the Dynamic and Temperature Fronts in the Scotia Sea and the Adjacent Water Areas. *Physical Oceanography*, 29(1), pp. 117–138. https://doi.org/10.22449/1573-160X-2022-2-117-138
23. Artamonov, Y.V., Lomakin, P.D. and Skripaleva, E.A., 2008. Seasonal and Interannual Variability of the characteristics of Scotia-Sea front based on the Satellite Measurements of Sea-Surface Temperature. *Physical Oceanography*, 18(1), pp. 52–62. https://doi.org/10.1007/s11110-008-9009-3
24. Artamonov, Yu.V., Skripaleva, E.A. and Nikolsky, N.V., 2020. Spatial Structure and Intra-Annual Variability of Weddell Sea Front Based on the Data of NOAA OI SST Reanalysis. *Ecological Safety of Coastal and Shelf Zones of Sea*, (4), pp. 89–102. https://doi.org/10.22449/2413-5577-2020-4-89-102 (in Russian).
25. Zuo, H., Balmaseda, M.A., Tietsche, S., Mogensen, K. and Mayer, M., 2019. The ECMWF Operational Ensemble Reanalysis-Analysis System for Ocean and Sea Ice: A Description of the System and Assessment. *Ocean Science*, 15(3), pp. 779–808. https://doi.org/10.5194/os-15-779-2019
26. Turner, J., 2004. The El Niño – Southern Oscillation and Antarctica. *International Journal of Climatology*, 24(1), pp. 1–31. https://doi.org/10.1002/joc.965
27. Turner, J., Colwell, S.R., Marshall, G.J., Lachlan-Cope, T.A., Carleton, A.M., Jones, P.D., Lagun, V., Reid, P.A. and Iagovkina, S., 2005. Antarctic Climate Change during the Last 50 Years. *International Journal of Climatology*, 25(3), pp. 279–294. https://doi.org/10.1002/joc.1130
28. Gong, D. and Wang, S., 1999. Definition of Antarctic Oscillation Index. *Geophysical Research Letters*, 26(4), pp. 459–462. https://doi.org/10.1029/1999GL900003

29. Wang, G. and Cai, W., 2013. Climate-Change Impact on the 20th-Century Relationship Between the Southern Annular Mode and Global Mean Temperature. *Scientific Reports*, 3, 2039. https://doi.org/10.1038/srep02039

30. Nikolskii, N.V., Artamonov, Y.V. and Skripaleva, E.A., 2023. Interannual Variability of Sea Surface Temperature at the Polar Latitudes of the Atlantic Ocean. *Gidrometeorologiya i Ekologiya*, 71, pp. 293–310. https://doi.org/1033933/2713-3001-2023-71-293-310 (in Russian).

31. Chapman, C.C., Lea, M.-A., Meyer, A., Sallee, J.-B. and Hindell, M., 2020. Defining Southern Ocean Fronts and their Influence on Biological and Physical Processes in a Changing Climate. *Nature Climate Change*, 10, pp. 209–219. https://doi.org/10.1038/s41558-020-0705-4

32. Lee, D.Y., Petersen, M.R. and Lin, W., 2019. The Southern Annular Mode and Southern Ocean Surface Westerly Winds in E3SM. *Earth and Space Science*, 6(12), pp. 2624–2643. https://doi.org/10.1029/2019EA000663

33. Thompson, D.W.J., Solomon, S., Kushner, P.J., England, M.H., Grise, K.M. and Karoly, D.J., 2011. Signatures of the Antarctic Ozone Hole in Southern Hemisphere Surface Climate Change. *Nature Geoscience*, 4, pp. 741–749. https://doi.org/10.1038/NGEO1296

34. Serykh, I.V. and Sonechkin, D.M., 2022. Link of El Niño – Southern Oscillation and Southern Annular Mode as Elements of Global Atmospheric Oscillation. *Vestnik of Saint-Petersburg University. Earth Sciences*, 67(4), pp. 614–630. https://doi.org/10.21638/spbu07.2022.404 (in Russian).

Submitted 17.12.2024; accepted after review 20.01.2025;
revised 17.09.2025; published 30.12.2025

About the authors:

Yuri V. Artamonov, Leading Research Associate, Marine Hydrophysical Institute of RAS (2 Kapitanskaya St., Sevastopol, 299011, Russian Federation), DSc (Geogr.), **ResearcherID: AAC-6651-2020**, **ORCID ID: 0000-0003-2669-7304**, *artam-ant@yandex.ru*

Elena A. Skripaleva, Senior Research Associate, Marine Hydrophysical Institute of RAS (2 Kapitanskaya St., Sevastopol, 299011, Russian Federation), PhD (Geogr.), **ResearcherID: AAC-6648-2020**, **ORCID ID: 0000-0003-1012-515X**, *sea-ant@yandex.ru*

Nikolay V. Nikolskii, Junior Research Associate, Marine Hydrophysical Institute of RAS (2 Kapitanskaya St., Sevastopol, 299011, Russian Federation), **ResearcherID: AAT-7723-2020**, **ORCID ID: 0000-0002-3368-6745**, *nikolsky.geo@gmail.com*

Contribution of the authors:

Yuri V. Artamonov – general scientific supervision of the study, statement of the study aims and objectives, method development, qualitative analysis of the results and their interpretation, discussion of the work results, conclusion drawing

Elena A. Skripaleva – review of literature on the study problem, qualitative analysis of the results and their interpretation, processing and description of the study results, discussion of the work results, conclusion drawing, preparation of the manuscript, text refinement

Nikolay V. Nikolskii – development and debugging of computer programmes for data processing, algorithm programming, graph plotting, participation in discussion of the article materials

All the authors have read and approved the final manuscript.